Neurobiology of Disease 129 (2019) 93–101

Contents lists available at ScienceDirect

Neurobiology of Disease

journal homepage: www.elsevier.com/locate/ynbdi

Cerebral aquaporin-4 expression is independent of seizures in tuberous sclerosis complex

Brittany Short[a], Lindsay Kozek[a,b], Hannah Harmsen[c], Bo Zhang[d], Michael Wong[d], Kevin C. Ess[a,b], Cary Fu[a], Robert Naftel[e], Matthew M. Pearson[f], Robert P. Carson[a,b,g,*]

[a] Department of Pediatrics, Division of Pediatric Neurology, Vanderbilt University Medical Center, United States
[b] Vanderbilt Brain Institute, Vanderbilt University, United States
[c] Department of Pathology, Vanderbilt University Medical Center, United States
[d] Departments of Neurology, Pediatrics, and Neuroscience, Washington University School of Medicine, United States
[e] Department of Neurosurgery, Vanderbilt University Medical Center, United States
[f] Neurosurgery, Sacred Heart Hospital, Pensacola, FL, United States
[g] Department of Pharmacology, Vanderbilt University Medical Center, United States

ARTICLE INFO

Keywords:
Aquaporin-4
Epilepsy
Tuberous sclerosis complex
Mouse

ABSTRACT

Astrocytes serve many functions in the human brain, many of which focus on maintenance of homeostasis. Astrocyte dysfunction in Tuberous Sclerosis Complex (TSC) has long been appreciated with activation of the mTORC1 signaling pathway resulting in gliosis and possibly contributing to the very frequent phenotype of epilepsy. We hypothesized that aberrant expression of the astrocyte protein aquaporin-4 (AQP4) may be present in TSC and contribute to disease pathology. Characterization of AQP4 expression in epileptic cortex from TSC patients demonstrated a diffuse increase in AQP4. To determine if this was due to exposure to seizures, we examined Aqp4 expression in mouse models of TSC in which *Tsc1* or *Tsc2* inactivation was targeted to astrocytes or glial progenitors, respectively. Loss of either *Tsc1* or *Tsc2* from astrocytes resulted in a marked increase in Aqp4 expression which was sensitive to mTORC1 inhibition with rapamycin. Our findings in both TSC epileptogenic cortex and in a variety of astrocyte culture models demonstrate for the first time that AQP4 expression is dysregulated in TSC. The extent to which AQP4 contributes to epilepsy in TSC is not known, though the similarities in AQP4 expression between TSC and temporal lobe epilepsy supports further studies targeting AQP4 in TSC.

1. Introduction

Tuberous Sclerosis Complex (TSC) is a multisystem neurodevelopmental disorder characterized most frequently by epilepsy, autism, psychiatric disorders, and varying degrees of developmental delay. Additionally, patients can have renal, cardiac, pulmonary, and dermatologic manifestations (Randle, 2017). Epilepsy in TSC is often severe and intractable, and when coupled with the challenges associated with autism, can be particularly disruptive.

Brain pathology in TSC is widespread and affects multiple cell types, including neurons, oligodendrocytes, and astrocytes. While the most marked abnormalities are seen within cortical tubers, more subtle abnormalities in myelination are appreciated diffusely (Simao et al., 2010). A primary role for astrocytes has been suspected in TSC with reactive astrocytes contributing to cortical tubers (Sosunov et al., 2008). A functional role of astrocytes in epilepsy in TSC is supported by the marked epilepsy phenotype seen in conditional mouse knockout models in which the primary cell type targeted was astrocytes (Uhlmann et al., 2002; Zhang et al., 2013).

Astrocytes serve multiple roles in the brain, including clearance of neurotransmitters, potassium regulation, metabolism of glutamate and ammonia to form glutamine, regulation of water homeostasis, and

Abbreviations: Aqp4, aquaporin-4; CaMKII, calmodulin-dependent protein kinase II; CKO, conditional knock-out; DIV, day *in vitro*; ERT, Cre fused to estrogen receptor; F/F, floxed/floxed; F/Wt, floxed/wild-type; GFAP, glial fibrillary acidic protein; GLT-1, glutamate transporter-1; GLAST, glutamate aspartate transporter; MGCM, mixed glia culture media; MRI, magnetic resonance imaging; mGluR5, metabotropic glutamate receptor 5; mTOR, mechanistic target of rapamycin; PBS, phosphate buffered saline; PI3K, phosphoinositide 3-kinase; PKC, protein kinase C; pS6, phosphorylated-S6 ribosomal protein; SEGA, subependymal giant cell astrocytoma; TLE, temporal lobe epilepsy; TSC, Tuberous Sclerosis Complex

* Corresponding author at: D-4105 MCN, 1161 21st Avenue South, Nashville, TN 37232-2594, United States.
E-mail address: robert.carson@vumc.org (R.P. Carson).

https://doi.org/10.1016/j.nbd.2019.05.003
Received 29 January 2019; Received in revised form 23 April 2019; Accepted 8 May 2019
Available online 09 May 2019
0969-9961/

formation and maintenance of a component of the blood-brain barrier (BBB). One protein which plays a key role in many of these astrocytic functions is the water channel aquaporin-4 (AQP4). While there are multiple aquaporins in the human body, AQP4 is the predominant astrocytic subtype. AQP4 has been shown to be expressed early in development in neuronal precursors, though with subsequent differentiation of neuronal progenitors, an astrocytic shift to AQP4 expression is seen (Cavazzin et al., 2006). Mouse studies have shown that Aqp4 is not required for viability, though Aqp4 loss results in impaired astrocyte migration to chemotactic stimuli, reduced glial scar formation and an increased seizure threshold (Papadopoulos and Verkman, 2008).

The contribution of astrocytes to epilepsy pathogenesis is increasingly appreciated and has been well reviewed in the context of temporal lobe epilepsy (de Lanerolle et al., 2010). Astrocytes in sclerotic lesions have been postulated to increase neuronal excitability through a variety of mechanisms including glutamate-dependent increases in extracellular K^+ due in part to changes in astrocyte morphology and cell swelling. Additionally, both AQP4 and blood-brain barrier dysfunction have been demonstrated to contribute to epileptogenesis. Leakage across the BBB has been shown to occur during acute epileptogenesis as well as during the chronic epileptic phase (van Vliet et al., 2007). Persistent leakage of serum IgG has been postulated to contribute to the neuronal dysfunction in temporal lobe epilepsy (Rigau et al., 2007). Additionally, AQP4-dependent mechanisms have been postulated to contribute to neuronal cell death in the hippocampus in eclampsia (Han et al., 2018) as well as altered water and K^+ homeostasis (Eid et al., 2005).

Given the marked abnormalities in astrocytes and evidence of BBB disruption in TSC (Boer et al., 2008a), we hypothesized that AQP4 is increased in brains of patients with TSC and may contribute to neuronal dysfunction and epilepsy in TSC. Herein we demonstrate expression changes in AQP4 in both TSC patient resected tissues as well as TSC mouse models, both demonstrating a marked upregulation of AQP4 in TSC.

2. Materials and methods

2.1. Human tissue

TSC patient (Table 1), age-matched cortical tissue from autopsy specimens (Table 2) and resected tissue from epilepsy patients (Table 3) were obtained with the assistance of the Vanderbilt University Medical Center pathology department. TSC and non-TSC epilepsy cortical tissue was obtained in the context of epilepsy surgery for the treatment of medically refractory epilepsy under Vanderbilt University IRB #130550. Tissue samples were paraffin embedded and cut into 5 μm sections. H&E sections were stained using established protocols by the Vanderbilt Translational Pathology core. Slides were deparaffinized followed by incubation in DPBS. Antigen retrieval was perform using 10 mM sodium citrate with 0.05% Tween-20, pH 6.0. Sections were subsequently blocked with 10% goat serum, 10% bovine serum albumin and 0.5% Triton-X100 in PBS (super-block) for 1 h at room temperature. Primary antibodies were diluted in super-block and incubated overnight at 4 °C. After washing with PBS, sections were probed with species appropriate secondary antibodies at 1:500 (anti-mouse, anti-rabbit, or anti-rat Alexa 488, 555, 647 fluorochromes, Invitrogen, Watham, MA, USA) for one hour at room temperature. Photomicrographs were obtained with an AMG Evos epifluorescence microscope (ThermoFisher, Watham, MA, USA). Slides were processed in parallel with all images obtained at 20× with identical light settings. Image analysis was performed with ImageJ (version 1.47, National Institutes of Health, Bethesda, MA, USA) and Adobe Photoshop CS5 (Adobe Systems, San Jose, CA, USA). Semi-quantitative alalysis of AQP4 expression from human samples was done through integration of the intensity of the 647 channel representing AQP4 across the entirety of the 20× photomicrograph. Primary antibody dilutions: GFAP 1:1000, phospho-S6 (Ser240–244) 1:200, (all Cell Signaling Technology, Danvers, MA, USA), and AQP4 1:500 (Alomone Labs 300–314, Jerusalem, Israel).

Table 2
Control, non-TSC patient cohort.

Age	Cause of death
8 days	Disseminated HSV-1 infection
2 years	Acute cardiac arrest
5 years	Pulmonary hemorrhage
10 years	Lymphocytic myocarditis
14 years	Sepsis
48 years	Cardiac sudden death

Table 3
Non-TSC epilepsy patient cohort.

Age at Resection	Resection location	Pathology
1 year	Right frontal	Focal cortical dysplasia, type IIB
12 years	Left temporal	Gliosis, hippocampal sclerosis
17 years	Left temporal	Neuronal heterotopia, hippocampal sclerosis

2.2. Mouse models

A conditional knockout mouse strain lacking *Tsc2* in glial progenitors was generated by breeding mice harboring a floxed *Tsc2* allele (Fu and Ess, 2013) to *Olig2-Cre* + mice (Jackson Laboratory #011103,

Table 1
TSC patient cohort.

Age at Resection	Gene mutation	Resection location	Pathology
8 days	*TSC2* point mutation	Right hemispherectomy	Balloon cells, microcalcifications
2.5 years	*TSC2* point mutation	Right temporo-occipital	Giant cells, decreased numbers of neurons, reactive astrocytosis, consistent with tuber
2.5 years	not done	Right frontal	Distorted neocortical architecture, balloon cells, loss of lamination, increased astrocytes, consistent with tuber
3 years	none detected	Left temporal lobe	Cytomegalic neurons, balloon cells, astrogliosis, calcification
3 years	not done	Right frontal	Disrupted lamination, dysmorphic neurons, balloon cells, reactive gliosis
4 years	*TSC2* frame shift	Right frontal and temporal	Hypomyelination and gliosis, large glassy GFAP+ and NeuN+ cells
6 years	not done	Left parietal	Reactive astrocytes, balloon cells, disrupted cortical lamination
6 years	*TSC2*	Right frontal	Deranged lamination, marked gliosis with focal calcification
9 years	*TSC1* frame shift	Right frontal	Disrupted lamination, cytomegalic neurons, balloon cells, hypomyelination with gliosis and calcification
13 years	not done	Left frontal	Reactive astrocytes, balloon cells, dysmorphic neurons, abnormal lamination
15 years	not done	Left frontal	Disorganized cortex, dysmorphic neurons, balloon cells, consistent with tuber
15 years	*TSC2* deletion	Right frontal	Consistent with tuber
48 years	*TSC1* frame shift	Left frontal	Balloon cells, reactive astrocytes, subcortical mineralization

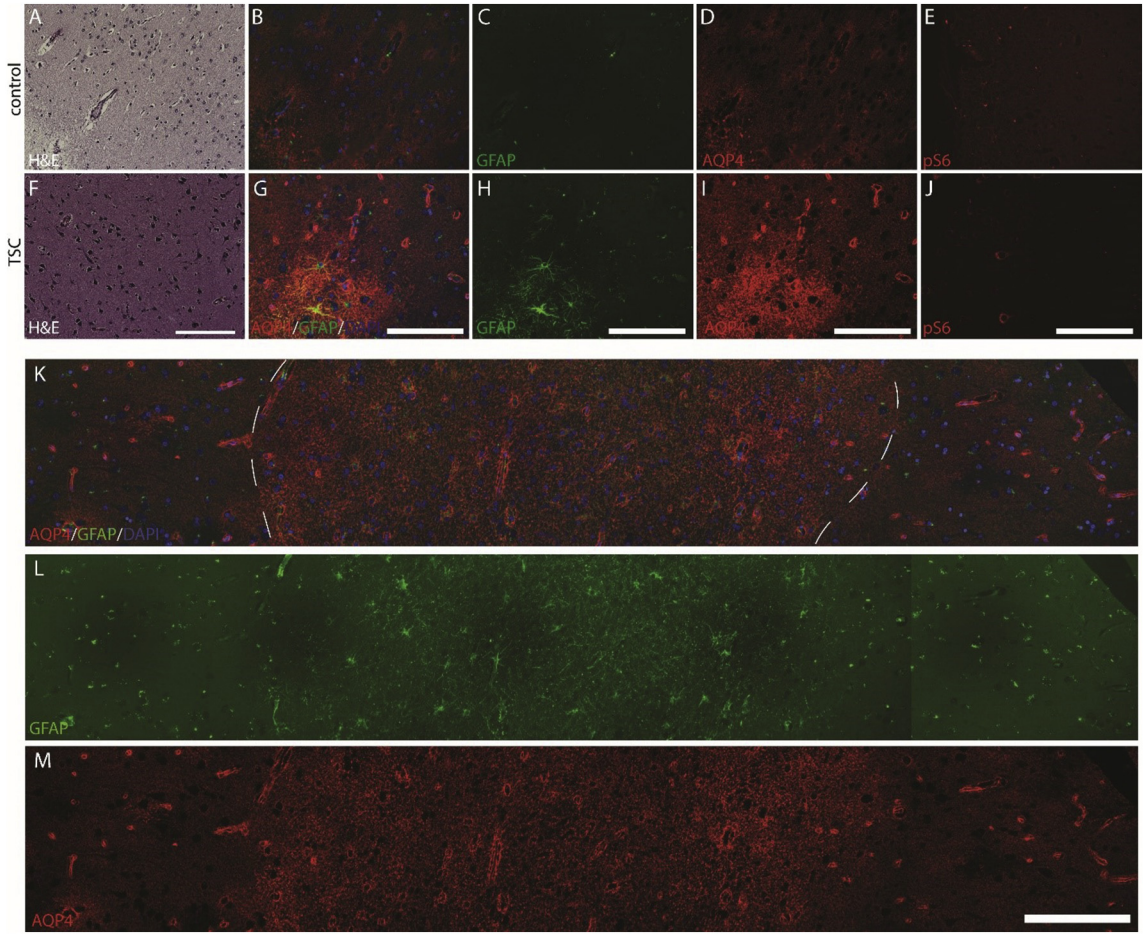

Fig. 1. Aquaporin-4 expression in TSC patient cortex. Representative 20× H&E sections from a 15 year-old patient with TSC and an age matched control (A, F). 20× photomicrographs of AQP-4 and GFAP in parallel cortical sections to the H&E sections in the control (B-D) and TSC patient (G-I) cortex. Demonstration of pS6 (serine 240/244) positive giant cells in TSC (J) but not control (E) parallel sections. Panoramic view of TSC cortex demonstrating an area of gliosis with diffuse AQP-4 immunoreactivity (demarcated by white line) surrounded by cortex with a more typical perivascular AQP-4 expression pattern (K-M). Scale bar = 200 μm.

Sacramento, CA, USA) as previously described (Carson et al., 2013). Subsequently, *Tsc2*$^{F/Wt}$*; Olig2*-Cre-positive mice were bred with homozygous *Tsc2*$^{F/F}$ mice to create animals homozygous for the *Tsc2* floxed allele (*Olig2-Tsc2* CKO). Similarly, mice transgenic for *ERT2*-Cre (Jackson Laboratory #008463, Sacramento, CA, USA) were bred with *Tsc2*$^{F/F}$ mice to create *Tsc2*$^{F/F}$*; ERT-Cre* (*ERT-Tsc2)* mice where *Tsc2* inactivation may be controlled temporally through exposure to tamoxifen. As tamoxifen was used *in vitro*, a breeding scheme where *ERT-Cre(+)Tsc2*$^{F/F}$ mice were crossed to *ERT-Cre(+)Tsc2*$^{F/F}$ mice was used to maximize output of homozygous *ERT-Cre(+)Tsc2*$^{F/F}$ pups. Genotyping was performed using PCR as previously described (Carson et al., 2013) See Supplemental Fig. 1C for primers used. GFAP-*Tsc1*-CKO astrocytes and P28 cortical tissue samples were generated as previously described (Uhlmann et al., 2002). All experiments were performed in both male and female animals using littermate controls whenever possible.

Mice were housed under normal environmental conditions with a standard 12-h light-dark cycle and *ad lib* access to water and food. Weekly weights were taken to ensure maintenance of normal food and water intake. Mice were euthanized under anesthesia for tissue harvesting, methods in accordance with AVMA guidelines. All work was conducted with the approval of the Institutional Animal Care and Use Committee (IACUC) at Vanderbilt University, Nashville, Tennessee (M/1600104) or at Washington University, St. Louis, Missouri (A-3381-01, 20160091).

2.3. Rapamycin treatment

Tsc2^{Olig2} mice were treated with 3 mg/kg rapamycin i.p. 5 days per week from P30-P60 and sacrificed at P60 as described previously (Carson et al., 2015). Rapamycin was stored at −20C as a 30 mg/ml stock solution in 100% ethanol then diluted in vehicle (0.25% Tween-20, 0.25% polyethylene glycol in PBS) prior to administration.

2.4. Immunofluorescence

Brain tissues were dissected from *Tsc2* CKO and littermate controls as previously described (Carson et al., 2013; Ess et al., 2005; Fu et al., 2011). Briefly, animals were anesthetized with ketamine/xylazine and perfused (P5 and older) with ice-cold phosphate buffered saline (PBS) followed by ice-cold 4% paraformaldehyde (PFA) in PBS (pH 7.4). Brains were post-fixed in 4% PFA overnight and cryoprotected in 30% sucrose prior to sectioning.

IF was performed with frozen sections as described above with paraffin-embedded human cortical tissue though antigen retrieval was not required in the frozen sections.

2.5. Immunoblotting

Mice were anesthetized with isoflurane and tissues rapidly dissected on ice, flash frozen in liquid nitrogen and stored at −80 °C. Lysate preparation, SDS-PAGE, and immunoblotting were performed as previously described (Grier et al., 2017). Primary antibodies: pS6 (Ser240/

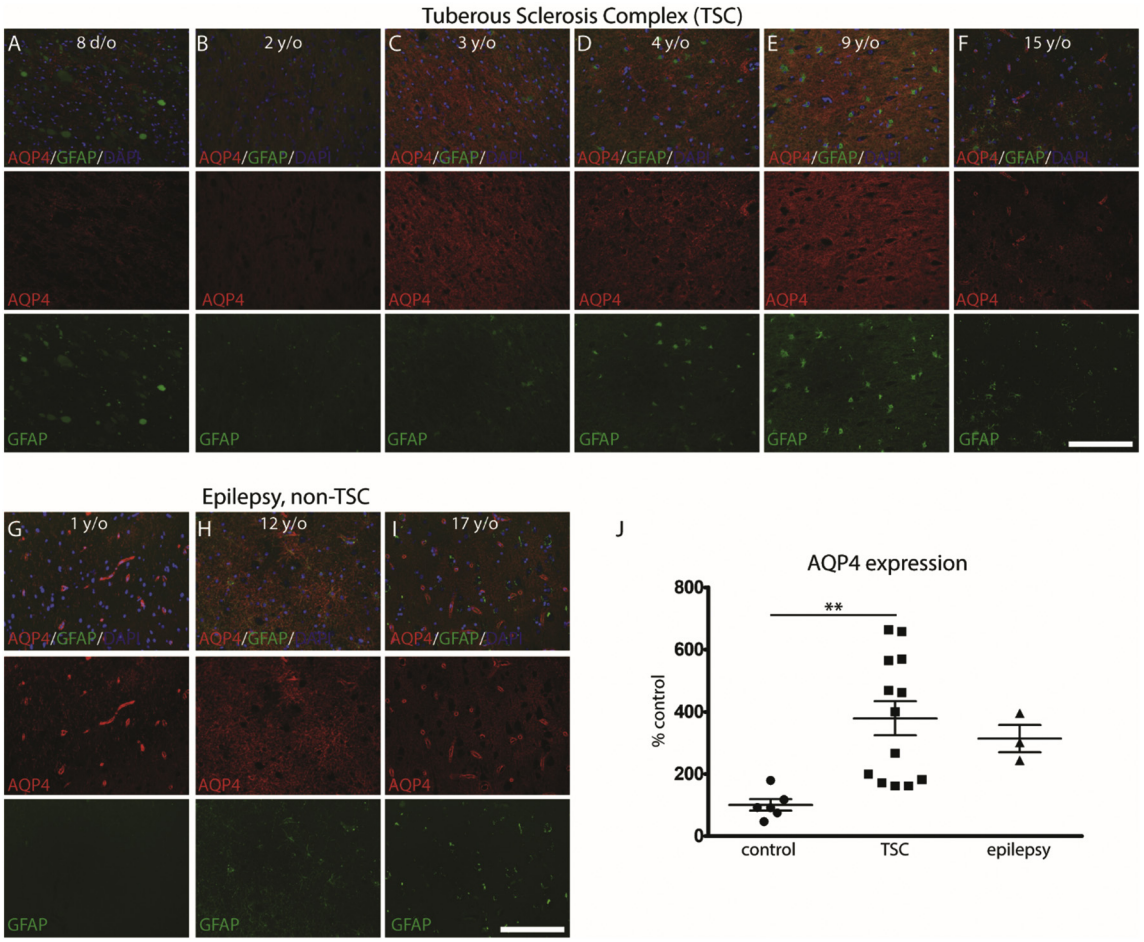

Fig. 2. Aquaporin-4 expression in TSC and non-TSC epilepsy patient cortex. 20× photomicrographs of AQP-4 and GFAP in cortical sections of TSC(A-F) and non-TSC epilepsy patient (G-I) cortex. Quantitation of AQP-4 signal intensity from control, TSC patient and non-TSC epilepsy cortical tissue (J). $p < .01$ by 1-way ANOVA with Tukey's post-test, $n = 6, 13, 3$. Scale bar = 200 µm.

244), GFAP and actin (Cell Signaling Technology, pS6 and GFAP 1:1000; actin 1:2000); Aqp4 1:500 (rabbit, Alomone Labs 300–314), and actin 1:2000 (mouse, Sigma, St. Louis, MO, USA).

2.6. Primary mouse astrocyte cultures

Primary mixed glial cultures were prepared from P0 to P2 mouse brains with modification of published protocols (Carson et al., 2015; O'Meara et al., 2011). Briefly, following euthanasia, cortical tissue was isolated, dissociated and plated into poly-L-lysine (PLL)-coated flasks incubated at 37 °C and 8.5% CO_2 in mixed glial culture media (MGCM) consisting of Dulbecco's modified Eagles medium (DMEM) with 10% fetal bovine serum (FBS), 1% penicillin/streptomycin, and 1% Glutamax (Gibco). Microglia and oligodendrocyte precursors were isolated and removed *via* differential shaking at day *in vitro* (DIV) 9. Astrocytes remaining in the T25 flask were washed with PBS and dissociated with 0.25% trypsin in Hanks' balanced salt solution (HBSS). Astrocytes were expanded through at least two passages prior to re-plating into flasks or onto poly-L-lysine-coated 24-well culture dishes and harvested 7 days later. For chronic rapamycin experiments, 1 day following plating, cells were treated with 20 nM rapamycin in DMSO vehicle or with DMSO alone.

For immunofluorescence microscopy, cells in 24-well plates were washed with PBS followed by fixation with 4% paraformaldehyde for 15 min. Following PBS washes, cells were processed for immunofluorescence as described above, prior to imaging with an Evos fluorescent microscope (AMG).

2.7. ERT treatment of astrocytes

In astrocytes possessing the ERT2 inducible Cre, 1 µM 4-OH tamoxifen (Sigma) in DMSO (tamoxifen) or DMSO vehicle were added to parallel cultures from the same animal, starting at DIV3 though DIV9. Astrocytes underwent differential shaking on DIV9 and were processed as described above. Loss of *Tsc2* was confirmed through PCR (Supplemental Fig. 1) and *via* immunoblot.

3. Results

To determine if AQP4 expression is altered in cortical brain tissue from patients with TSC, AQP4 expression was characterized from brain tissue obtained from TSC patients during epilepsy surgery (Table 1). Patients ranged from 8 days to 48 years of life at the time of resection. Five patients demonstrated mutations in *TSC2*, two with mutations in *TSC1*; one patient had no mutation identified. Five patients did not have documented genetic testing. In all cases, pathology was consistent with that expected in TSC, including the presence of giant cells, dysmorphic neurons, distorted neocortical architecture and gliosis. Paraffin-embedded sections from TSC patients, age-matched controls (Table 2), and non-TSC epilepsy patients (Table 3) were co-labeled with antibodies against AQP4 and GFAP with parallel sections probed with phosphorylated S6 (Serine 240/244) and stained with hematoxylin and eosin (H&E) (Fig. 1). As predicted, cortical GFAP expression and S6 phosphorylation (Serine 240/244) were increased in TSC samples. In addition to the expected perivascular localization, AQP4 expression was

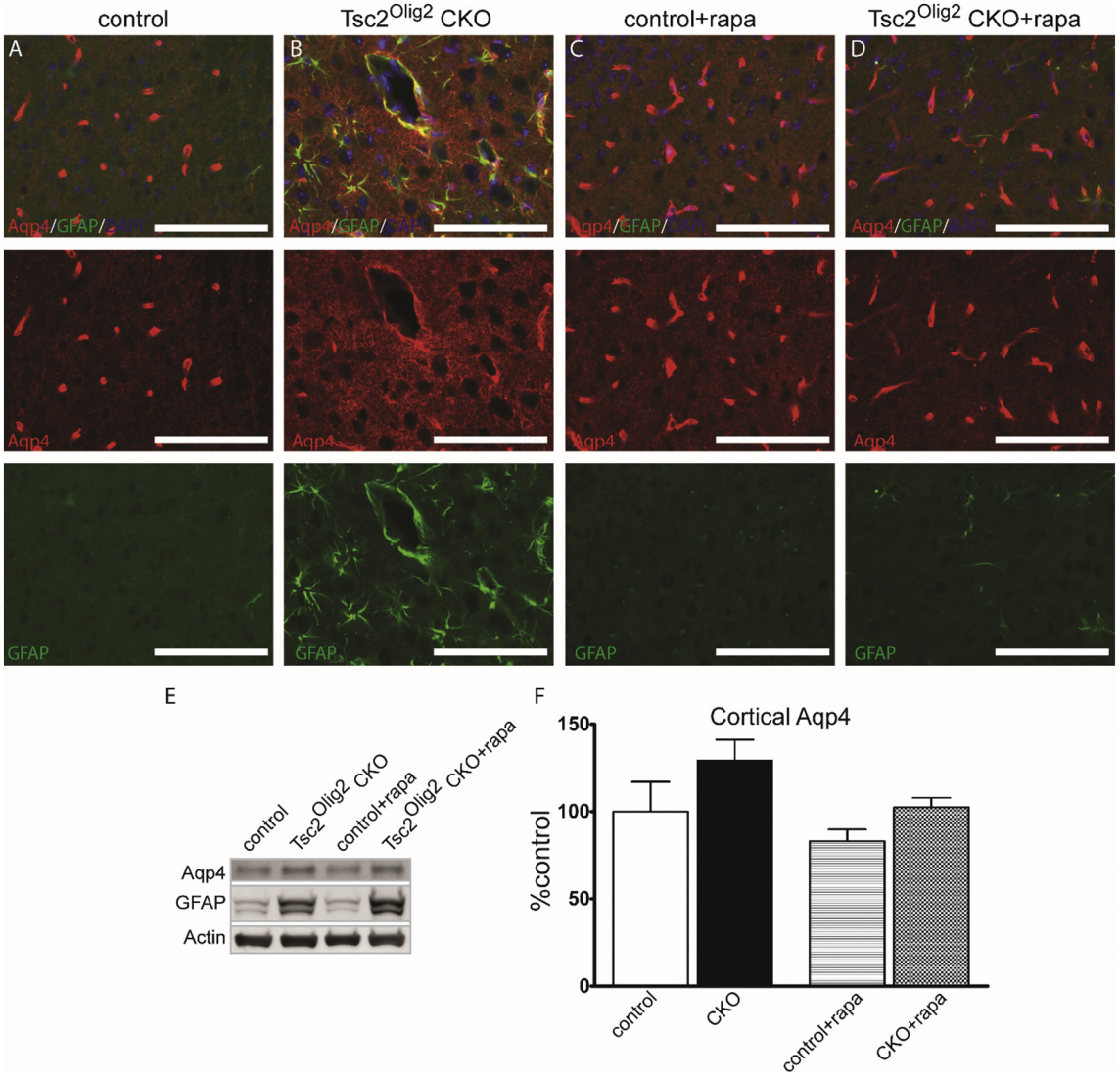

Fig. 3. Aquaporin-4 expression in the $Tsc2^{Olig2}$ CKO mouse model. 20× photomicrographs of Aqp-4 and GFAP expression are demonstrated with immunofluorescence and immunoblotting in the $Tsc2^{Olig2}$ CKO mouse model in which Tsc2 is targeted to glial precursors before (A-B, *E*-F) and after (C-D, E-F) treatment with rapamycin. Means compared with 1-way ANOVA with Tukey's multiple comparison test, $n = 3$ animals per group. Scale bar = 200 μm.

diffusely increased in all the TSC patient samples. Within TSC specimens, regions with diffuse AQP4 expression demonstrated increased gliosis and decreased organization, whereas in flanking regions a more normal appearing perivascular AQP4 expression pattern was seen (Supplemental Fig. 2).

As our controls were from non-epilepsy pathologic specimens, to contrast the increase in AQP4 in TSC to non-TSC epileptic tissue, we examined resected cortical tissue from patients with focal epilepsy of other causes. AQP4 expression in non-TSC epileptic tissue was increased relative to control specimens but did not reach the high levels of expression seen in many of the TSC specimens (Fig. 2). Similar to that seen in the TSC samples, the AQP4 expression varied within specimens and was increased in association with regions of gliosis and dysplastic cortex (Supplemental Fig. 3). A semi-quantitative evaluation of total AQP4 signal intensity across the entirety of images from control, TSC and non-TSC epileptic cortex demonstrated that AQP4 expression was increased in all patient specimens but with marked variability within TSC samples.

Given that the AQP4 expression was increased in many of the human TSC brain specimens beyond that seen in the non-TSC epileptic cortex, we sought to determine if the increased AQP4 expression may be due to cell autonomous mechanisms in astrocytes. To determine if increased Aqp4 expression is due to loss of Tsc2 (Han et al., 2018), Aqp4 expression was examined at P60 in brain sections and cortical extracts from our previously described $Tsc2^{Olig2}$-CKO mouse model (Carson et al., 2015) with immunofluorescence and immunoblotting, respectively (Fig. 3). In the $Tsc2^{Olig2}$-CKO mouse model, *Tsc2* is conditionally inactivated in glial precursors resulting in deletion in both oligodendrocytes and in astrocytes. Clinical seizures have not been observed in this model. Similar to the findings in human cortical tissue, Aqp4 expression demonstrated the expected perivascular localization in all samples and similar to that seen in the TSC patient samples, its expression was more diffuse throughout the CKO cortex. As has been described previously, gliosis was evident with increased expression of GFAP in the CKO cortex. When quantitated by immunoblotting, a trend towards increased Aqp4 expression was seen in the CKO mice but this was not statistically significant. A similar trend was seen with immunoblotting of cortical extracts from P28 $Tsc1^{GFAP}$ CKO mice (Supplemental Fig. 4), a well-characterized epileptic mouse model of TSC in which GFAP-Cre is used to target *Tsc1* ($Tsc1^{GFAP}$) in astrocytes (Zhang et al., 2013). Given the important role of mTORC1 activation in TSC, we asked whether Aqp4 expression may be modified by treatment with rapamycin. Aged-matched control and $Tsc2^{Olig2}$-CKO mice were treated with rapamycin from P30 to P60 as previously described (Carson et al.,

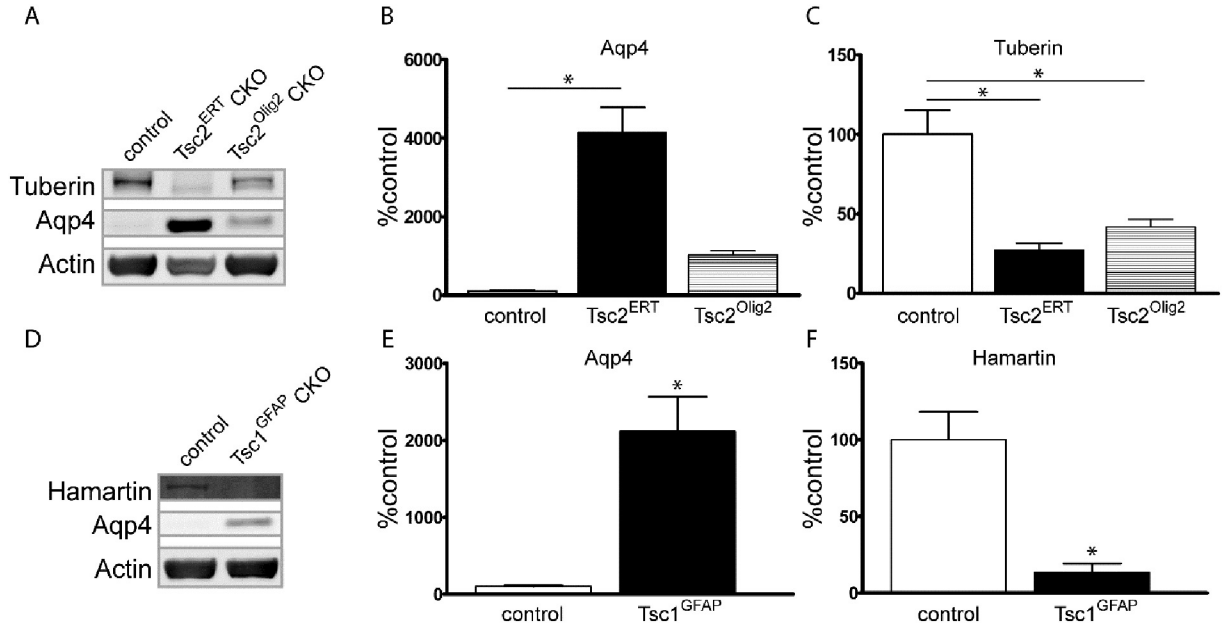

Fig. 4. Increased Aqp-4 expression in Tsc2 and Tsc1 deficient astrocytes. Aqp-4 expression was characterized by immunoblotting in primary cultures of astrocytes derived from the $Tsc2^{Olig2}$ CKO mouse model (A-C), a novel tamoxifen-inducible $Tsc2^{ERT}$ CKO model (A-C), and the $Tsc1^{GFAP}$ CKO mouse model (D-F). *$p < .05$. Means compared with 1-way ANOVA with Tukey's multiple comparison test (C) and Student's *t*-test (E). $n = 3$–4 independent cultures per group.

2015). Following treatment with rapamycin, Aqp4 expression was not as diffuse and returned to the expected perivascular expression pattern. When evaluated by immunoblotting, the overall Aqp4 expression appeared slightly decreased after treatment with rapamycin, but overall Aqp4 expression was not significantly different across groups. These findings mirror those seen in the TSC patient samples and suggest that a component of the increase in Aqp4 expression is mTORC1-dependent and not due to seizure exposure.

To further characterize the association between mTORC1 activation and Aqp4 expression in astrocytes and to determine if changes in Aqp4 are the result of cell autonomous changes within astrocytes, we utilized primary astrocyte cultures from the established TSC mouse models described above (Carson et al., 2015; Uhlmann et al., 2002), as well as in a novel *Tsc2*^{ERT} Cre mouse line we developed. To quantify Aqp4 expression in Tsc2-deficient astrocytes, lysates of primary astrocyte cultures were evaluated by immunoblotting (Fig. 4A-C). Aqp4 expression trended towards but was not significantly increased in astrocyte extracts derived from the *Tsc2*^{Olig2}-CKO mouse, consistent with the *in vivo* data. Previous studies with red fluorescent protein lineage tracing using the Ai14 mouse suggested that a majority of cortical astrocytes are targeted by Olig2-Cre (Carson et al., 2015, Fig. S4), however the residual tuberin expression seen on the western blot suggests incomplete targeting of astrocytes.

Given the possibility that Olig2-Cre may not target all cortical astrocytes, we also generated a novel inducible ERT-Cre *Tsc2* (*Tsc2*^{ERT}) model to further characterize the interaction between tuberin loss and Aqp4 expression. *Tsc2*^{ERT} astrocyte cultures derived from mouse pups homozygous for floxed alleles of Tsc2 were treated with vehicle (DMSO) or 4-hydroxy-tamoxifen (tamoxifen) to create *Tsc2* null astrocytes. Following treatment with tamoxifen, Aqp4 expression was markedly increased in *Tsc2*^{ERT} cultures. The degree of tuberin loss was more pronounced in the *Tsc2*^{ERT} cultures than in the $Tsc2^{Olig2}$ derived cultures. A lower molecular weight tuberin band was seen in the *Tsc2*^{ERT} culture which manifests as a doublet in the *Tsc2*^{Olig2} culture, a band consistent with residual expression of tuberin lacking the GAP domain. In aggregate, these data demonstrate a significant inverse correlation between tuberin expression and Aqp4 expression, further supporting such an association between the two proteins ($r = -0.7127$, $p = .0472$).

To determine if the increase in Aqp4 expression was specifically associated with *Tsc2* loss or may also be associated with loss of *Tsc1* (encodes hamartin), Aqp4 expression was quantified in primary astrocyte cultures derived from the *Tsc1*^{GFAP} CKO mouse. Similar to the results in the *Tsc2*^{ERT} astrocytes lacking tuberin, Aqp4 expression was also markedly increased in astrocytes lacking hamartin (Fig. 4D-F), supporting that loss of either tuberin or hamartin may lead to elevated Aqp4 expression.

As demonstrated earlier, Aqp4 expression is markedly increased in *Tsc2* deficient astrocytes (Fig. 5). Following chronic treatment of *Tsc2*^{ERT} astrocyte cultures for 6 days with rapamycin, Aqp4 expression was significantly decreased, though did not completely normalize to control values despite suppression mTORC1 activity as demonstrated with decreased S6 phosphorylation (Supplemental Fig. 5). These findings suggest a role for mTORC1 activation in modulation of Aqp4 expression but also suggests other mechanisms may be contributing to the increased expression of Aqp4.

In addition to the cytomegaly seen in *Tsc2*-deficient astrocytes, large cystic-appearing vacuolar structures were frequently seen in the *Tsc2*-deficient astrocyte cultures which were not appreciated in control cultures (Fig. 6). Immunofluorescence staining of the astrocytes with GFAP and actin demonstrate that the vacuole-like structures exhibit GFAP expression both along the border of and within the vacuole, supporting that they are intracellular. To determine if the vacuoles are associated with mTORC1 activation, we conducted time-lapse imaging of *Tsc2*^{ERT} astrocytes that were treated acutely with 100 nm rapamycin for 24 h, a dose demonstrated to reduce astrocyte cell size with acute treatment (Supplemental Fig. 6). These studies demonstrated a decrease in vacuole size and number, demonstrating a sensitivity of these structures to treatment with rapamycin.

4. Discussion

Given the multifaceted role for astrocytes in TSC pathology and BBB dysfunction, we hypothesized that expression of the astrocyte protein AQP4 may be altered in TSC and contribute to disease pathology. In cortical tissue resected from TSC patients in the context of epilepsy surgery, we demonstrate a markedly increased expression of AQP4. The marked and diffuse increase in AQP4 expression is not unprecedented.

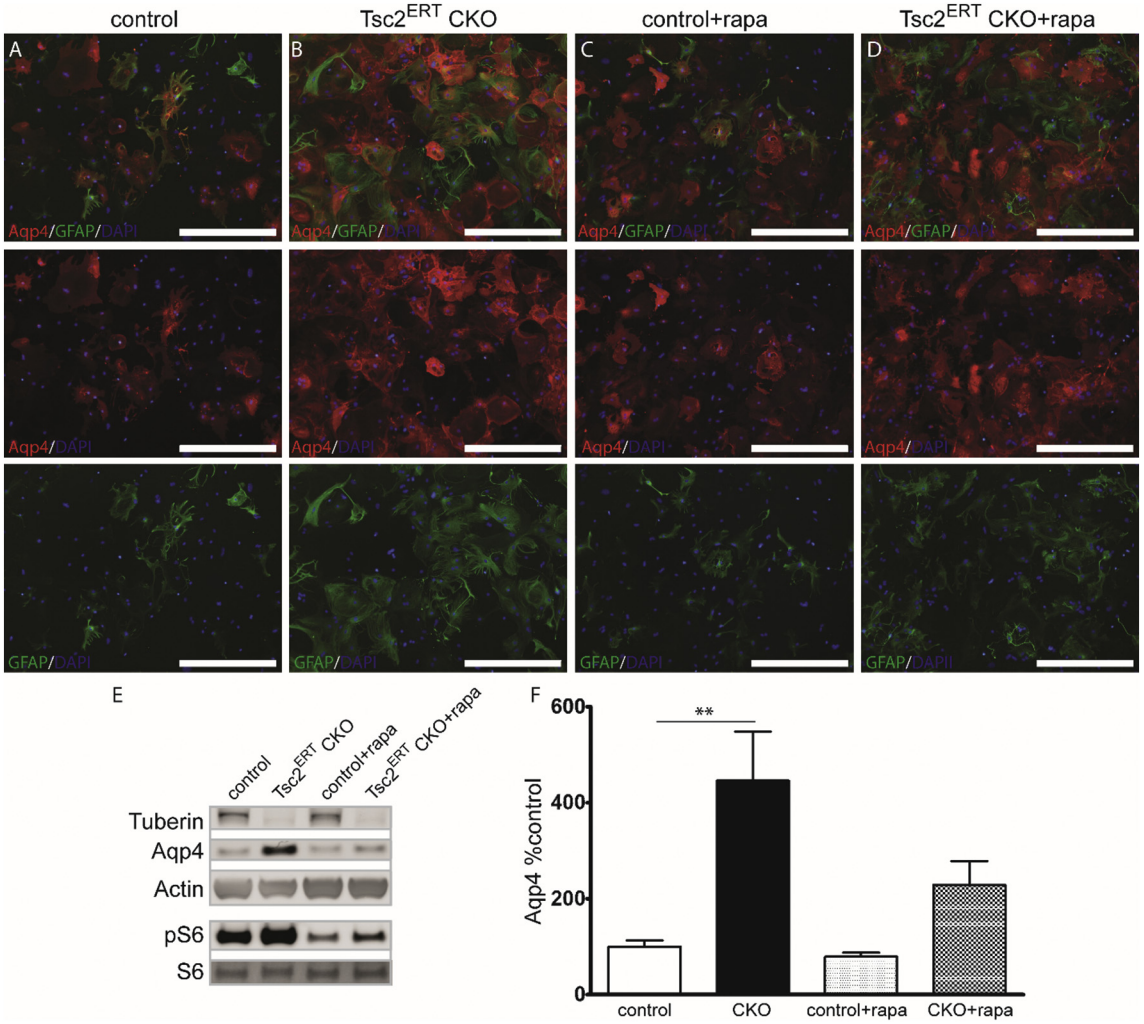

Fig. 5. mTORC1 sensitivity of Aqp-4 expression. Aqp-4 and GFAP expression were characterized with immunofluorescence and immunoblotting in primary cultures of astrocytes derived from the tamoxifen inducible Tsc2^{ERT} CKO model before (A-B, *E*-F) and after treatment with rapamycin (C—F). 10× photomicrographs, scale bar = 400 μm. $^{**}p < .01$ for genotype effect only. Means compared with 2-way ANOVA with Bonferroni's post-test, $n = 5–6$ independent cultures per group.

Increases in AQP4 expression have been previously reported in temporal lobe epilepsy, with mRNA analyses as well as with immunohistochemistry showing diffusely increased AQP4 expression similar to what we report in TSC and confirmed in our non-TSC epilepsy specimens (Lee et al., 2007). Likewise, diffusely increased AQP4 expression has been reported in tumors as well as in Alzheimer's disease, diseases that are also associated with gliosis (Moftakhar et al., 2010; Noell et al., 2015).

To address whether the increased AQP4 is related to seizure burden, we additionally examined expression in cultured mouse astrocytes lacking Tsc1 or Tsc2. Cultured astrocytes demonstrated increased Aqp4 expression which was inversely proportional to tuberin expression. The increased Aqp4 expression in primary cultures supports that seizure exposure is not the sole etiology of increased AQP4 expression in the epileptic TSC cortex. This finding, in combination with the decrease in Aqp4 expression following treatment with rapamycin, supports a role for mTORC1 activation increasing Aqp4 expression. The lack of a marked increase in Aqp4 expression in cortical tissue extracts may be due in part to a dilution effect from not targeting other cell types or may suggest altered localization of Aqp4. The lack of ability to directly compare effects of loss of Tsc1 and Tsc2 using the same Cre-driver is a limitation of our study. The marked increased in AQP4 expression and transition from a more normal perivascular localization to a more diffuse presentation was noted within different regions of individual samples, including with the non-TSC epilepsy cohort. This was most notable in a specimen which included a type IIB cortical dysplasia, a type of malformation characterized by giant cells with increased mTOR activity (Majolo et al., 2018), further supporting a link between mTOR activation and AQP4 expression.

There are several mechanisms by which AQP4 expression and BBB disruption may be linked to TSC and mTORC1 signaling. AQP4 expression is modulated by CaMKII and PKC, kinases whose activity and expression are modulated by mTOR. In addition, Shi et al. demonstrated a role for mGluR5 stimulation in glutamate-dependent astrocyte swelling which was shown to be blocked by mGluR5 antagonism or a siRNA directed against AQP4 (Shi et al., 2017). In addition to Gαq-dependent mechanisms, mGluR5 induces activation of the PI3K/Akt/mTOR signaling pathway (Olmo et al., 2016). Increased mGluR5 expression in tubers and SEGAs in TSC (Boer et al., 2008b) further suggests a mechanism by which glutamate acting through mGluR5 may synergize with mTOR signaling to increase AQP4 expression in TSC. The cystic structures in the *Tsc2*-deficient cultured astrocytes appear similar to the vacuoles described by Guo, Zou, and Wong in astrocytes after kainic acid-induced seizures (Guo et al., 2017), but a clear association with Aqp4 expression has not yet been determined.

The degree to which AQP4 contributes to disease pathology and epilepsy in TSC is not known. AQP4 is highly expressed in the endfeet of perivascular astrocytes where it makes up a component of the blood

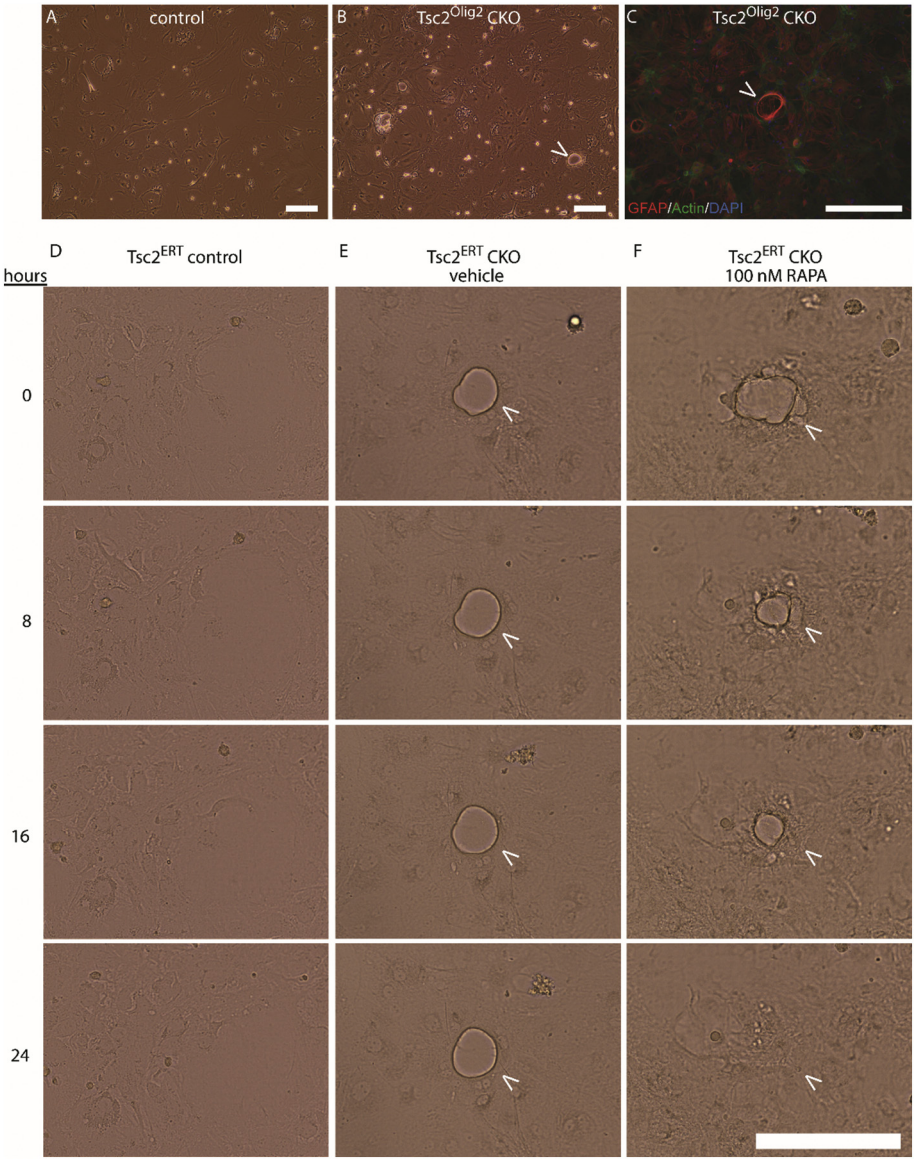

Fig. 6. Intracellular vacuoles in Tsc2 deficient astrocytes. Bright field (A-B) and immunofluorescence (C) photomicrographs of GFAP positive intracellular vacuoles in Tsc2 deficient astrocytes. Scale bar = 200 um Phase contrast time-lapse imaging of vacuoles following vehicle (E) or rapamycin treatment (F) for 24 h. Scale bar 100 um.

brain barrier. Evidence for a disrupted blood-brain barrier along with activated microglia has been previously reported in pathologic specimens from TSC patients (Boer et al., 2008a). Our findings demonstrate both an association between gliosis and AQP4 expression and suggest impairment in the perivascular targeting of AQP4. AQP4 dysregulation is thought to contribute to epileptogenesis by allowing leakage of serum proteins across the BBB and altering water and K^+ homeostasis (Eid et al., 2005; Han et al., 2018; Rigau et al., 2007; van Vliet et al., 2007), potentially contributing to the peritubер focal epileptogenicity associated with TSC. This role may be further supported by MRI studies demonstrating increased water diffusion in the brains of TSC patients, with marked increases in diffusion in perilesional white matter (Garaci et al., 2004). An overall increase in water diffusion in the cortex *versus* in the cerebellum has been postulated to be due in part to the relative increase in cortical expression of GLAST and AQP4 in the cortex. Additional data has implicated AQP4 in the enhanced swelling of cortical astrocytes after glutamate exposure (Han et al., 2004), suggesting another mechanism by which AQP4 dysregulation may contribute to the increased diffusion signal on MRI seen in TSC. The extent to which diffusion changes in TSC are due to dysmyelination or due to increased expression of AQP4 is not known. DTI imaging studies of either mouse or human brains which can differentiate radial *versus* axial diffusion may be used to help define the contribution of the respective cell types and quantitate responses to pharmacologic agents which may modify either myelination or AQP4 expression.

When contrasted to findings in temporal lobe epilepsy, the increase in AQP4 expression in TSC is consistent with multiple lines of evidence supporting a role for astrocyte dysfunction in both temporal lobe epilepsy and in TSC. In addition to changes in AQP4 expression, altered glutamatergic signaling is seen in both TLE and TSC. As noted, increased expression of astrocytic mGluR5 has been reported in TSC. Similar findings in temporal lobe epilepsy have been reported and extended to include increased expression of ionotropic glutamate receptors (Das et al., 2012). Glutamatergic signaling, in both TLE and TSC, may be further amplified through decreased astrocytic expression of glutamate transporters GLT-1 and GLAST, functionally increasing extracellular glutamate (Albrecht and Zielinska, 2017; Wong et al., 2003).

AQP4 expression is tightly associated with Kir potassium channels in astrocytes, channels which demonstrate decreased expression in TSC and TLE(Djukic et al., 2007; Jansen et al., 2006). The impaired ability to remove potassium from the extracellular space coupled with a decrease in extracellular space secondary to AQP4-dependent cell swelling, may further impede neuronal repolarization (Albrecht and Zielinska, 2017; Xu et al., 2009). While studies have demonstrated an increased seizure threshold in *Aqp4* null mice, Lee et al. demonstrated an increase in seizure frequency in *Aqp4* null mice *versus* controls following kindling of the hippocampus with kainic acid (Lee et al., 2012). Thus, future studies will be required to determine the extent to which the increase in AQP4 expression in TSC contributes to cortical epileptogenesis and whether similar mechanisms are seen in the hippocampus.

5. Conclusions

Despite continued development of medications for the treatment of epilepsy, one in three patients with epilepsy remains drug resistant (Chen et al., 2017). Intractable epilepsy in patients with TSC remains a major contributor to morbidity and affects quality of life for patients and their families. Identification of novel drug targets and mechanisms remains key to development of new therapies for the treatment of epilepsy. The similarities between increased AQP4 expression in TLE and our data demonstrating increased expression of AQP4 in TSC supports the hypothesis that AQP4 contributes significantly to disease pathology and epilepsy in TSC. Further studies are needed to both define the exact mechanisms by which loss of TSC alters AQP4 expression as well as the extent to which modulation of AQP4 expression or function can alter network excitability in TSC. Should AQP4 expression be shown to alter network excitability in TSC, approaches which target either AQP4 expression or function may serve as novel therapeutic strategies for the treatment of epilepsy in TSC.

Funding

This work was supported by the National Institutes of Health K08 NS083710 to RPC and.

R01 NS056872 to MW.

Appendix A. Supplementary data

Supplementary data to this article can be found online at https://doi.org/10.1016/j.nbd.2019.05.003.

References

Albrecht, J., Zielinska, M., 2017. Mechanisms of excessive extracellular glutamate accumulation in temporal lobe epilepsy. Neurochem. Res. 42, 1724–1734.
Boer, K., et al., 2008a. Clinicopathological and immunohistochemical findings in an autopsy case of tuberous sclerosis complex. Neuropathology 28, 577–590.
Boer, K., et al., 2008b. Cellular localization of metabotropic glutamate receptors in cortical tubers and subependymal giant cell tumors of tuberous sclerosis complex. Neuroscience 156, 203–215.
Carson, R.P., et al., 2013. Deletion of Rictor in neural progenitor cells reveals contributions of mTORC2 signaling to tuberous sclerosis complex. Hum. Mol. Genet. 22, 140–152.
Carson, R.P., et al., 2015. Hypomyelination following deletion of Tsc2 in oligodendrocyte precursors. Ann. Clin. Transl. Neurol. 2, 1041–1054.
Cavazzin, C., et al., 2006. Unique expression and localization of aquaporin-4 and aquaporin-9 in murine and human neural stem cells and in their glial progeny. Glia 53, 167–181.
Chen, Z., et al., 2017. Treatment outcomes in patients with newly diagnosed epilepsy treated with established and new antiepileptic drugs: a 30-year longitudinal cohort study. JAMA Neurol. 75 (3), 279–286.
Das, A., et al., 2012. Hippocampal tissue of patients with refractory temporal lobe epilepsy is associated with astrocyte activation, inflammation, and altered expression of channels and receptors. Neuroscience 220, 237–246.
de Lanerolle, N.C., et al., 2010. Astrocytes and epilepsy. 7, 424–438.
Djukic, B., et al., 2007. Conditional knock-out of K(ir)4.1 leads to glial membrane depolarization, inhibition of potassium and glutamate uptake, and enhanced short-term synaptic potentiation. J. Neurosci. 27, 11354–11365.
Eid, T., et al., 2005. Loss of perivascular aquaporin 4 may underlie deficient water and K + homeostasis in the human epileptogenic hippocampus. In: Proceedings of the National Academy of Sciences of the United States of America. vol. 102. pp. 1193–1198.
Ess, K.C., et al., 2005. Developmental origin of subependymal giant cell astrocytoma in tuberous sclerosis complex. Neurology 64, 1446–1449.
Fu, C., Ess, K.C., 2013. Conditional and domain-specific inactivation of the Tsc2 gene in neural progenitor cells. Genesis 51, 284–292.
Fu, C., et al., 2011. GABAergic interneuron development and function is modulated by the Tsc1 gene. Cereb. Cortex 22, 2111–2119.
Garaci, F.G., et al., 2004. Increased brain apparent diffusion coefficient in tuberous sclerosis. Radiology 232, 461–465.
Grier, M.D., et al., 2017. Loss of mTORC2 signaling in oligodendrocyte precursor cells delays myelination. PLoS One 12, e0188417.
Guo, D., et al., 2017. Rapamycin attenuates acute seizure-induced astrocyte injury in mice in vivo. Sci. Rep. 7, 2867.
Han, B.C., et al., 2004. Regional difference of glutamate-induced swelling in cultured rat brain astrocytes. Life Sci. 76, 573–583.
Han, X., et al., 2018. Changes in the expression of AQP4 and AQP9 in the Hippocampus following eclampsia-like seizure. Int. J. Mol. Sci. 19.
Jansen, L., et al., 2006. Epileptogenesis and Reduced Inward Rectifier Potassium Current in Tuberous Sclerosis Complex-1-Deficient Astrocytes.
Lee, T.S., et al., 2007. Gene expression in temporal lobe epilepsy is consistent with increased release of glutamate by astrocytes. Mol. Med. 13, 1–13.
Lee, D.J., et al., 2012. Decreased expression of the glial water channel aquaporin-4 in the intrahippocampal kainic acid model of epileptogenesis. Exp. Neurol. 235, 246–255.
Majolo, F., et al., 2018. MTOR pathway in focal cortical dysplasia type 2: what do we know? Epilepsy Behav. 85, 157–163.
Moftakhar, P., et al., 2010. Aquaporin expression in the brains of patients with or without cerebral amyloid angiopathy. J. Neuropathol. Exp. Neurol. 69, 1201–1209.
Noell, S., et al., 2015. Water channels aquaporin 4 and −1 expression in Subependymoma depends on the localization of the tumors. PLoS One 10, e0131367.
Olmo, I.G., et al., 2016. Dissecting the signaling pathways involved in the crosstalk between metabotropic glutamate 5 and cannabinoid type 1 receptors. Mol. Pharmacol. 90, 609.
O'Meara, R.W., et al., 2011. Derivation of enriched oligodendrocyte cultures and oligodendrocyte/neuron myelinating co-cultures from post-natal murine tissues. J. Vis. Exp. 54, 1–9.
Papadopoulos, M.C., Verkman, A.S., 2008. Potential utility of aquaporin modulators for therapy of brain disorders. Prog. Brain Res. 170, 589–601.
Randle, S.C., 2017. Tuberous sclerosis complex: a review. Pediatr. Ann. 46, e166–e171.
Rigau, V., et al., 2007. Angiogenesis is associated with blood–brain barrier permeability in temporal lobe epilepsy. Brain 130, 1942–1956.
Shi, Z., et al., 2017. Aquaporin 4-mediated glutamate-induced astrocyte swelling is partially mediated through metabotropic glutamate receptor 5 activation. Front. Cell. Neurosci. 11, 116.
Simao, G., et al., 2010. Diffusion tensor imaging of commissural and projection white matter in tuberous sclerosis complex and correlation with tuber load. Am. J. Neuroradiol. 31, 1273–1277.
Sosunov, A.A., et al., 2008. Tuberous sclerosis: a primary pathology of astrocytes? Epilepsia 49 (Suppl. 2), 53–62.
Uhlmann, E.J., et al., 2002. Astrocyte-specific TSC1 conditional knockout mice exhibit abnormal neuronal organization and seizures. Ann. Neurol. 52, 285–296.
van Vliet, E.A., et al., 2007. Blood–brain barrier leakage may lead to progression of temporal lobe epilepsy. Brain 130, 521–534.
Wong, M., et al., 2003. Impaired glial glutamate transport in a mouse tuberous sclerosis epilepsy model. Ann. Neurol. 54, 251–256.
Xu, L., et al., 2009. Impaired astrocytic gap junction coupling and potassium buffering in a mouse model of tuberous sclerosis complex. Neurobiol. Dis. 34, 291–299.
Zhang, B., et al., 2013. Vigabatrin inhibits seizures and mTOR pathway activation in a mouse model of tuberous sclerosis complex. PLoS One 8.